I&EC research
Industrial & Engineering Chemistry Research
pubs.acs.org/IECR
Article

Heat-Integrated Pervaporation–Distillation Hybrid System for the Separation of Methyl Acetate–Methanol Azeotropes

Chuanxin Zong, Qingkai Guo, Bowen Shen, Xiaoquan Yang, Haoli Zhou,* and Wanqin Jin*

Cite This: *Ind. Eng. Chem. Res.* 2021, 60, 10327–10337

ABSTRACT: Pervaporation is typically considered an energy-efficient technology for the separation of azeotropic mixtures. However, the vaporization of the permeate leads to a temperature drop in the residual stream, and a supply of external energy is required to maintain a constant residual stream temperature in traditional pervaporation processes, which lowers their energy efficiency. Therefore, in this study, a heat-integrated pervaporation–distillation hybrid system was designed and investigated for the separation of an azeotropic MeAc–MeOH mixture using a low-temperature residual stream to cool the top vapor of the column. The temperature drop in the residual stream during pervaporation was studied using simulations and experiments. Pervaporation–distillation hybrid processes with and without heat integration were simulated and compared with special distillation under various operating parameters; their energy efficiencies were also compared. The results indicated that pervaporation–distillation with heat integration can lower the energy consumption by 24% compared to that via pressurized distillation with heat integration. Additionally, the energy efficiency increased by 31.7% compared to that by pressurized distillation with heat integration at a MeAc feed concentration of 50 wt %. The system proposed in this study is simple and practical for the energy-efficient design of pervaporation setups in industrial settings.

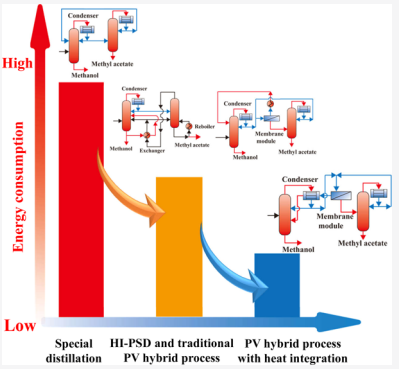

1. INTRODUCTION

The energy consumed in separation processes is critical to their industrial application because it is estimated to account for as much as 55% of the total energy consumed by the separation industry.[1] Therefore, a large amount of energy can be saved with the development and application of high-energy efficient technologies. Membrane technologies, such as pervaporation (PV), are energy-efficient when the membrane shows good selectivity, which is beneficial for reducing energy consumption. Hence, the use of PV for azeotrope separation after optimization is known to reduce the energy consumption to some extent compared to special distillation[2] because the separation principle in PV follows the solution-diffusion model instead of vapor–liquid equilibrium. This implies that PV can effortlessly break up the azeotropic point without increasing the temperature or pressure, which is known to occur in distillation. Moreover, the energy required for PV involves the enthalpy of evaporation for the permeate and not the energy required to heat the entire feed solution. Paredes et al.[3] estimated the operating cost of each unit with the aid of conceptual models for the separation of a methyl acetate–methanol (MeAc–MeOH) mixture using a membrane-distillation hybrid technology. Their results indicated that the introduction of PV in the hybrid process can reduce the total operational cost.

However, during PV, the evaporation of the permeate decreases the temperature of the residual stream when the value of the stage cut (which is defined as the mass ratio of the permeate and feed stream[4]) is high because of the evaporation enthalpy of the permeate.[5] Therefore, external heat is typically supplied to maintain the temperature of the residual stream, which results in an increase in the energy consumption. Simultaneously, the condensation of the permeate vapor also increases the energy consumption. Repetitive heating enhances energy consumption.[6] Therefore, the energy efficiency can be further improved using a low-temperature residual stream to condense the permeate or the top vapor stream during distillation in the PV–distillation hybrid system.[7] The present study aimed to enhance the energy efficiency of the PV–distillation hybrid process for MeAc production via heat transfer between the PV and distillation processes. To the best of our knowledge, this is the first study where the energy recycling was simulated using a low-temperature residual stream to condense the top vapor stream of the distillation column.

MeAc, which is an important green bulk chemical, is extensively used in the flavor and fragrance industries because of its low toxicity and relatively low environmental impact.[8,9]

Received: April 24, 2021
Revised: June 21, 2021
Accepted: June 23, 2021
Published: July 7, 2021

https://doi.org/10.1021/acs.iecr.1c01513
Ind. Eng. Chem. Res. 2021, 60, 10327–10337

Among the various chemical methods that have been proposed for the synthesis of MeAc in industrial settings,[10,11] esterification is popular because of its relative ease of use.[12−14] However, the addition of excess MeOH during esterification inevitably results in the separation of MeOH and MeAc.[15] Moreover, the direct formation of an azeotrope consisting of 82.5 wt % MeAc and 17.5 wt % MeOH makes its separation via simple distillation even more difficult.[16] Therefore, special distillation methods, such as extractive distillation, are utilized to obtain high-purity MeAc.[16,17] However, because of the relatively high energy consumption in extractive distillation, the exploration of a new technique, or a coupled technique with a higher energy efficiency, is required to achieve the separation of MeAc−MeOH azeotropes. A reduction in the energy consumption will eventually support the economy, environment, and industrial development.[18]

Studies on the simulation of energy consumption during the separation of MeAc−MeOH mixtures, particularly on the PV−distillation hybrid process, are scarce. Steinigeweg et al.[19] investigated the separation of a MeOH−MeAc azeotropic mixture using a hybrid process of PV and reactive distillation. However, PV was regarded as a part of the hybrid technology only to overcome the distillation boundary and optimize the total energy consumption of the technology under a specific feed concentration; the energy consumed in PV as part of the hybrid process was not considered. Other studies on the assessment of PV have mostly focused on breaking the balance of the azeotropic point to reduce the operating cost, without considering the energy consumption during PV.[20−23] Furthermore, variations in feeding properties, such as concentration or membrane separation capacity, can cause deviations between simulations and the actual process.[24] Therefore, it is important to include various operating parameters in the simulations to ensure similarities with the actual process.

In this study, a polydimethylsiloxane (PDMS) ceramic membrane was employed to separate the MeAc−MeOH mixtures; this membrane exhibited a higher flux and separation factor compared to those of other commercial MeAc-selective membranes.[25,26] In addition, membranes with MeOH selectivity show low flux, which leads to an increase in the membrane area and incurs high investment cost.[3] The heat transfer during PV was studied using experiments and calculations, which proved that the heat required for PV was primarily based on the energy supplied by the vacuum pump and feed stream. The energy consumption of the PV−distillation hybrid process with heat integration and that of extractive and pressurized distillation were calculated using Aspen Plus. The effects of various feed conditions on the distillation process were also investigated to minimize the energy consumption. Finally, simulations of the energy consumption under different feed conditions, such as feed concentrations, membrane separation capacities, and membranes with different separation factors, were considered to determine the optimal operating conditions.

2. EXPERIMENT AND SIMULATION

2.1. Experiment. An ∼1.5 μm-thick PDMS/ceramic composite membrane was fabricated in our laboratory; this membrane was previously tested for the separation of a MeAc−MeOH mixture;[25,27] the experimental data were discussed in a previous work[25] and only used for simulation here. The detailed calculation process of the separation performance is shown in Supporting Information. Two thermometers were placed at the feed and residual sides of the membrane model to measure the temperature drop during PV, and the energy supplied by the vacuum pump was measured using a three-phase digital electric power meter.

2.2. Simulations. The simulations were performed using Aspen Plus software (Aspen Tech). The nonrandom two-liquid (NRTL) model was applied to calculate the parameters of the mixtures, such as activity coefficients, because it is suitable for the calculation of miscible nonelectrolyte systems such as the MeAc−MeOH mixture.[28] The binary NRTL parameters are presented in Table S2. Distillation, condenser, and vacuum pump models were employed according to previous reports.[29,30] The simulations of PV were performed, and the effects of the operating parameters on PV were determined using a traditional model.[29]

2.2.1. Model of the PV Process. The mathematical model of the PV process is rather complicated.[31] For this reason, the black-box modeling method is an appropriate choice.[31] A user-defined PV unit operation model developed in Aspen Plus based on mass and energy balances was employed to establish the black-box model. Owing to the tubular module applied in the industry, the mixtures flowing through the membrane surface can be recognized as a one-dimensional (1D) plug flow model to ease the calculation in the simulation. In the 1D plug flow model, the detailed membrane process is recognized as a black box that only needs information about the input and output streams[3] (detailed information is provided in Supporting Information).

2.2.2. Heat Exchanger and Vacuum. The heat transfer system was simulated using the HeatX model in Aspen Plus. A dry vacuum pump was used for this process. The vapor mixture on the permeate side condensed before reaching the vacuum pump. After condensation, the liquid was sent to column two. The energy consumption of the vacuum pump was calculated based on the assumption of an ideal isentropic process as follows[30]

$$P_S = \frac{k}{k-1} q_{V,in} p_{in} \left[\left(\frac{p_{out}}{p_{in}} \right)^{k-1/k} - 1 \right] \quad (1)$$

where k is the isentropic exponent, P_S is the isentropic power, $q_{v,in}$ represents the volume of vapor in the permeate side, and p_{in} and p_{out} represent the pressures of import and export, respectively.

2.2.3. Temperature Drop in the Residual Stream. The vaporization of permeate mixtures requires energy derived from the feed stream if no extra energy is supplied. The temperature of the residual stream (as shown in Figure S1) decreases, according to the energy balance in this system.[29] Simultaneously, the temperature of the feed and residual streams can significantly affect the membrane performance. Therefore, a different empirical formula has been proposed to predict the temperature drop of the residual stream[3,6,29,32] and relate it to the membrane performance to optimize the process design.

$$T_r = T_f - (\Delta H_{vap} F_p - W_{pump})/c_{p,r} \quad (2)$$

where T_r and T_f represent the temperatures of the residual and feed streams, respectively, ΔH_{vap} is the vaporization enthalpy, W_{pump} is the energy supplied by the pump, and $c_{p,r}$ is the heat capacity of the residual stream. The heat of vaporization and

https://doi.org/10.1021/acs.iecr.1c01513
Ind. Eng. Chem. Res. 2021, 60, 10327−10337

heat capacity were estimated by Aspen Plus using the analysis run mode.

2.2.4. Energy Efficiency. Energy efficiency is a key characteristic of the separation process. As mentioned earlier, the energy consumption required for the separation of azeotropic mixtures using different processes was simulated and compared in this study. Equation 3 was used for the evaluation of the PV process under the assumption of a reversible, infinitely slow process. This implies that the minimum work of separation for a binary mixture depends on the change in the chemical potential in the binary mixtures.

$$-W_{\min} = -RT(x_i \ln(\gamma_i x_i) + x_j \ln(\gamma_j x_j)) \quad (3)$$

where x represents the mole fraction, γ represents the activity coefficient, and subscripts i and j represent the components of the mixture.

To estimate the total efficiency of the various processes, the energy efficiency (η) was considered for comparing the ratio of the ideal to the actual energy consumption, as shown in eq 4. W_{actual} represents the energy consumption of the actual process and is calculated as the sum of heating and cooling duties in the separation process, which depends on the operating conditions, equipment performance, and process design.

$$\eta = \frac{W_{\min}}{W_{\text{actual}}} \quad (4)$$

2.2.5. Distillation Process. The properties and binary parameters of the mixtures in the distillation process were obtained using Aspen Plus, and specifically the NRTL model, over the entire studied temperature range.[5] For simplicity, the pressure drop corresponding to each column was neglected.[3] The Murphree tray efficiency can be affected by many factors such as the contact time of the liquid and vapor on the tray, tray style, and physical properties of the materials.[34] Murphree tray efficiencies from 0.7 to 1.05 have been reported.[35] To simplify the calculation, a mean value of 0.85 was used in the simulation. The MeAc concentration of the top stream from column one was estimated as 81 wt %. In addition, the MeAc concentration of the top stream from column two was estimated to be 83.5 wt %, which was used to estimate the distillate rate of columns one and two. The optimization of both distillation processes was conducted according to three variables: the number of theoretical stages, location of the feed stage, and reflux ratio. The sensitivity of the model analysis tools in Aspen Plus was used to minimize the energy consumption of the entire process. It is well known that an increase in the theoretical stages reduces the energy consumption of the distillation column. Hence, the optimal number of theoretical stages was considered as the case when the relative energy consumption difference was lower than 0.5% by increasing the number of theoretical stages with an extra stage. The following optimization procedure determines the location of the feed stage. The preferred feed stage is where the energy consumption of the reboiler is the lowest.[33]

2.2.6. Hybrid Process. Figure 1 shows the flowsheet of the hybrid PV−distillation process. The feed stream was introduced into the distillation column, where the MeAc−MeOH azeotropic mixture and over 99 wt % MeOH were obtained at the top and bottom of the column, respectively. Two azeotropic streams from two columns were mixed and condensed in the top condenser (phase separator) of column one and subsequently fed to the membrane module to facilitate

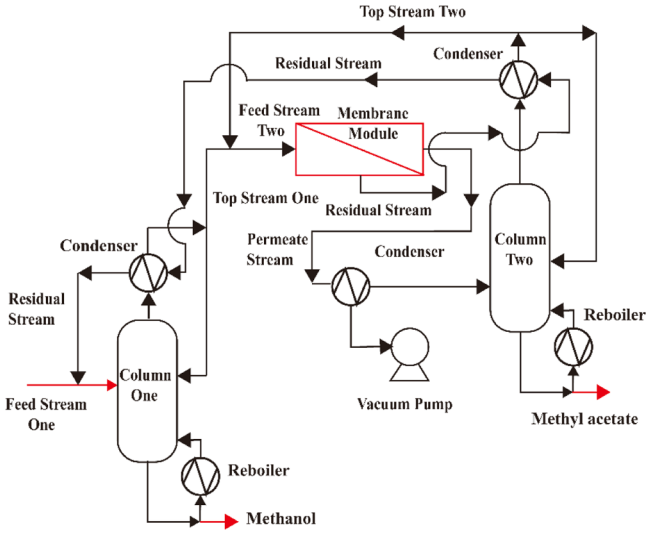

Figure 1. Flowsheet of the hybrid PV−distillation process.

the breakup of the azeotropic composition of the MeAc−MeOH mixture. The nonazeotropic permeate stream (vapor phase) of the membrane was directed into column two for further separation, which resulted in 99 wt % MeAc at the bottom and a MeAc−MeOH azeotropic mixture at the top of the column. A low-temperature nonazeotropic (residual) stream from the membrane was used as a refrigerant in the condensers of both columns because of the enthalpy of evaporation of the permeate.[5] After heat transfer, the residual stream was recycled back into column one for further separation.

3. RESULTS AND DISCUSSION

3.1. Model Verification. It is necessary to validate the model describing the PV process before performing the simulations. The data presented in our previous study were used in the present study to simulate the PV process.[25] The proposed model for the PV process was investigated by simulating the effect of feed concentration on the membrane performance, as shown in Figure 2. The degree of consistency between the experimental and predicted data was observed to be acceptable because R^2 was over 0.95, confirming the accuracy of the model.

3.2. Temperature Drop in the Residual Stream. As previously mentioned, the temperature drop in the residual stream is related to the stage cut. When the stage cut was <0.01, the temperature difference between the inlet and outlet of the membrane module was <0.3 °C, indicating that the effect of this temperature change can be neglected. However, a further increase in the stage cut led to the transportation of a higher number of separated species through the membrane, which implies that more energy was required for their evaporation, resulting in a large temperature drop in the residual stream, as shown in Figure 3. Therefore, if the stage cut is too high and no external energy is supplied, a severe temperature drop can drastically weaken the membrane performance.[6] Several studies have suggested that external heat is required for the conventional PV unit, which consists of several membrane modules in series, to maintain a constant temperature for the residual stream and consequently maintain an adequate membrane performance, which also affects its energy efficiency.[6] To enhance the energy efficiency of the

https://doi.org/10.1021/acs.iecr.1c01513
Ind. Eng. Chem. Res. 2021, 60, 10327−10337

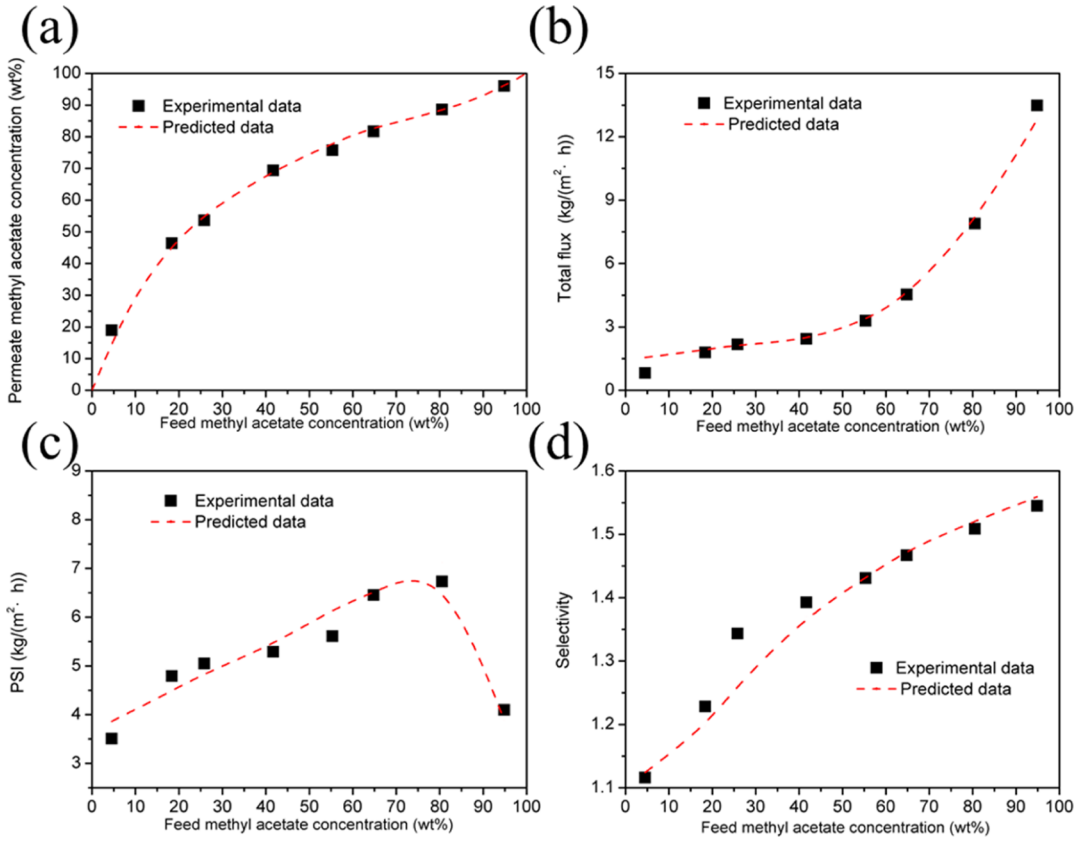

Figure 2. Predicted and experimental data of (a) permeate concentrations, (b) total fluxes, (c) PV separation index (PSI), and (d) selectivity at different feed compositions (the membrane performance tests were conducted at 50 °C, the permeate pressure was fixed at 5 kPa, and the feed flow was fixed at 1000 mL/min).

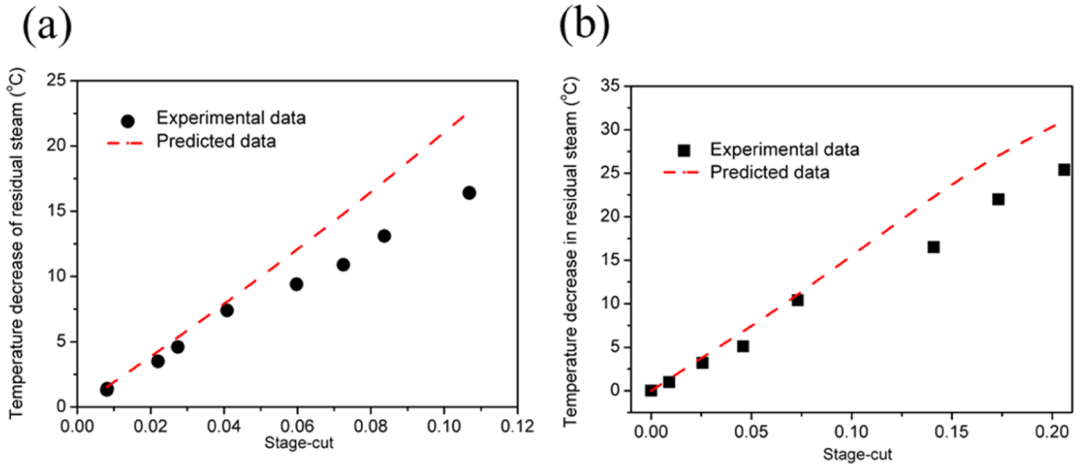

Figure 3. Temperature drops in the residual stream at different stage cuts with different substrates and isentropic exponents. (a) MeOH (η = 1.23) and (b) MeAc (η = 1.10). (The tests of membrane performance were conducted at 23 °C. The permeate pressure is fixed at 5 kPa, and the feed flow is fixed at 1000 mL/min).

membrane, the energy balance should be evaluated by considering the low-temperature residual stream as the refrigerant of the condenser at the top of the column.[36] Thus, a low supply of external energy is required in this case, which can lead to higher energy efficiency. Therefore, accurate prediction of the temperature drop in the residual stream should be prioritized because it can be used to guide the design of energy-efficient processes in industrial settings.

Figure 3 shows the simulated temperature drop of the residual stream at different stage cut values. A higher stage cut was observed to lead to a higher temperature drop in the residual stream because of permeate evaporation. Furthermore, when the value of the stage cut increased, the difference between the experimental and predicted data increased, but R^2 was only 0.67. This was because when the stage cut was ~0.14, the temperature of the residual stream decreased from ~25 to ~0 °C, indicating an inevitable heat exchange with the environment, leading to a larger difference between experimental and predicted data.

https://doi.org/10.1021/acs.iecr.1c01513
Ind. Eng. Chem. Res. 2021, 60, 10327−10337

Figure 4 shows the results of heat transfer between the membrane module and the environment, which were used to determine the heat transfer coefficient K via simulations. The environmental temperature was 23 °C, and the initial temperature of the solution in the membrane module was set to 45 °C. The heat transfer coefficient was calculated by integrating the curve in Figure 4, as 397 W/(m^2·°C). Subsequently, the predicted temperature drop of the residual stream was calculated (the calculation method is shown in Supporting Information).

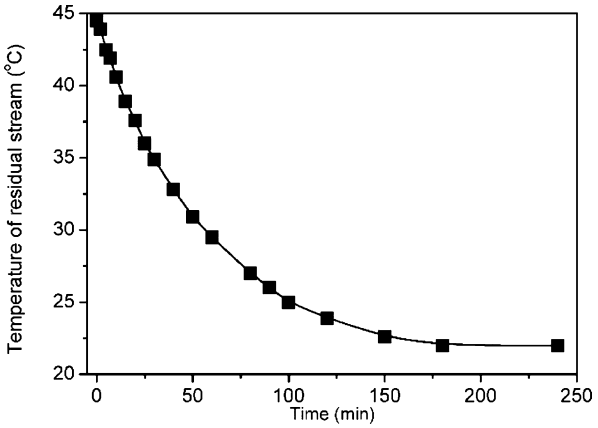

Figure 4. Dependence of the temperature change of the mixture on time (without PV). The feed material is MeAc, the total mass weight is 2.5 kg, the environmental temperature is 23 °C, and the initial temperature is 45 °C.

The decreasing temperature curves of the residual stream with different stage cuts and separated species after module optimization are shown in Figure 5. The predicted data were in good agreement (R^2 > 0.9) with the experimental data presented in Figure 3, which confirms that the feed stream, vacuum pump, and heat transfer with the environment can affect the temperature drop in the residual stream. Heat transfer with the environment can be neglected if thermal insulation is applied because the heat transfer coefficient without thermal insulation was obtained as 397 W/(m^2·°C) in our experiment, whereas that in industrial settings is ∼30 W/(m^2·°C).[37] This indicates that the temperature loss from the heat transfer with the environment represents less than 5% of the total energy consumption for vaporization. Hence, in the simulation process, the energy consumption for vaporization was considered to occur mainly from the vacuum pump and feed material.

Vacuum is known to be favorable for the evaporation of liquids at a specific temperature;[32] however, achieving a low-vacuum environment requires a high amount of energy, according to eq 1. Figure 6 shows the effect of vacuum pressure on the energy consumption of the PV process, which was obtained by simulating PV involving 100 kg of the permeate mixture at different permeate pressures in an ideal isentropic process using a dry pump. In this simulation, the liquid-to-vapor expansion under vacuum conditions was assumed to be adiabatic expansion.[38] The expansion energy of the separated species decreased with increasing permeate pressure. This is a result of the relationship between the expansion energy and permeate pressure, as expressed in eq 1. The outlet pressure of the pump was the same as the atmospheric pressure, and the isentropic exponent slightly changed. Therefore, an increase in inlet pressure was observed to lead to a decrease in the expansion energy.

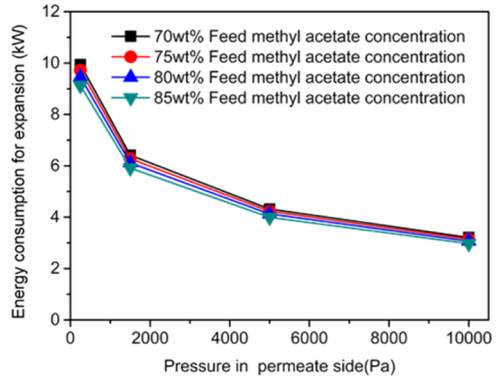

Figure 6. Energy consumption of the vacuum pump with various feed concentrations and permeate pressures. (The simulation was conducted at 50 °C. The feed flow is fixed at 1000 mL/min. and the permeate mass flow is fixed at 100 kg/h.)

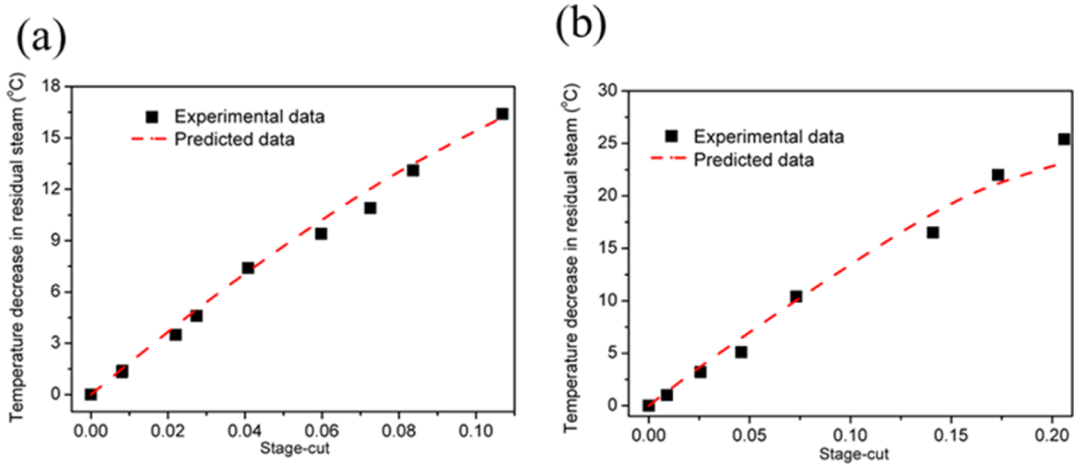

Figure 5. Temperature drop of the residual stream at different stage cuts with (a) MeOH and (b) MeAc after optimization. (The tests of membrane performance were conducted at 23 °C. The permeate pressure is fixed at 5 kPa, and the feed flow is fixed at 1000 mL/min.)

https://doi.org/10.1021/acs.iecr.1c01513
Ind. Eng. Chem. Res. 2021, 60, 10327−10337

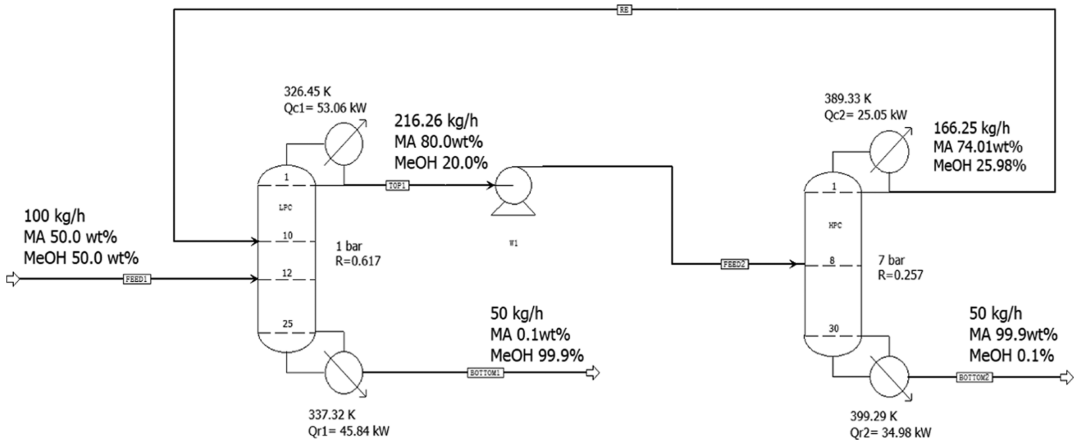

Figure 7. Optimal pressurized distillation process for MeAc−MeOH separation.

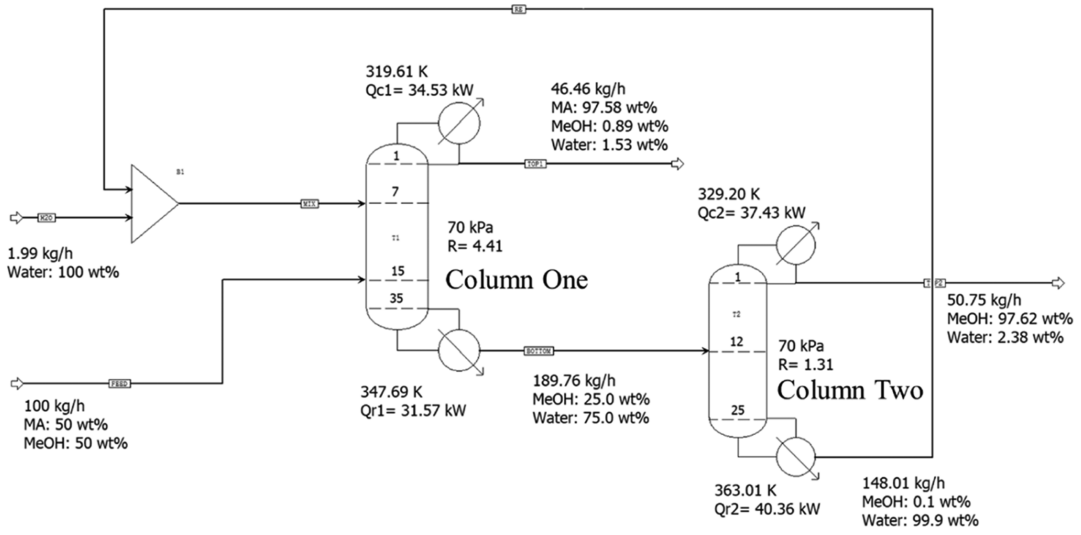

Figure 8. Optimal extractive distillation process for MeAc−MeOH separation.

Figure 6 also shows a slight decrease in the energy of expansion with an increase in the MeAc feed rate. This can be ascribed to the lower concentration of MeOH on the permeate side, because its isentropic exponent (1.225) was slightly higher than that of MeAc (1.103). Equation 1 predicts a higher energy consumption of the vacuum pump at higher values of the isentropic exponent, which indicates that for a lower temperature drop of the component, less external energy should be supplied to maintain a constant temperature of the feed stream for the component with a higher isentropic exponent.

3.3. Simulation. *3.3.1. Extractive and Pressure Distillations.* The flowsheet of the extensively used pressurized distillation process is illustrated in Figure 7.[39] The feed flow rate was fixed at 100 kg/h with a MeAc concentration of 50 wt %; it was first introduced into the common distillation unit to obtain over 99 wt % MeOH in the bottom stream. The azeotropic stream at the top of column one was fed to column two to obtain over 99 wt % MeAc at the bottom of column two. The top stream, whose composition was slightly lower than that of the azeotropic mixture, was sent back to column one to facilitate circulation. The pressurized column two was maintained at 7 bar to minimize the energy consumption throughout the process because a high pressure in column two would reduce the life of the Raschig rings and increase the costs.[40] The specifications of the different streams and equipment are shown in Figure 7. The simulated energy in this case was 158.93 kW/100 kg, which was similar to that in a previous work (~152.9 kW/100 kg).[39] The direct heat integration of pressurized distillation was also investigated (detailed information is shown in Figure S3); the energy consumption was 108.83 kW, which significantly decreases the energy consumption of separation. However, the increasing pressure in column two, the high temperature of the condenser and the reboiler in column two, and the complex heat transfer process also led to extra investment cost of a distillation column.

As shown in Figure 8, extractive distillation also requires two common columns to separate the MeAc−MeOH mixture, which simplifies the whole process and diminishes the investment cost. Although water is useful to be employed as the extractant to separate the azeotropic mixtures as reported,[41,42] it also affects the purity of products and limits the application of extractive distillation. The simulation results revealed that the energy consumption throughout the process was high which equals 143.89 kW/100 kg and was similar to that reported in a previous work (~146.2 kW/100 kg).[41]

3.3.2. Hybrid Process with the PV Unit. A membrane with a separation factor of 1.95 and a flux of 8.5 kg/(m^2·h) for the PV

https://doi.org/10.1021/acs.iecr.1c01513
Ind. Eng. Chem. Res. 2021, 60, 10327−10337

of the MeAc−MeOH azeotropic mixtures at 50 °C and 5 kPa permeate pressure was employed in this simulation.

In the hybrid process, the vapor fractions of the residual stream and feed stage can affect the energy consumption of column one.[23] These effects were investigated, and the results are shown in Figure 9. When the feed was in the tenth stage, the energy consumption of column one was the lowest. The energy consumption decreased with an increase in the vapor fraction of the residual stream because of the reduced energy consumption of the reboiler.

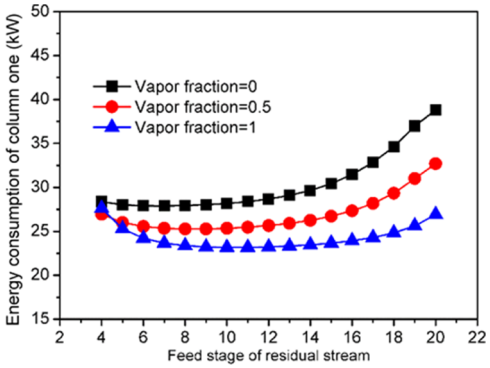

Figure 9. Effect of residual stream and feed stage on the energy consumption of column one with various vapor fractions (feed concentration: 50 wt %, stage cut: 0.8, and feed flow rate: 100 kg/h).

Figure 10 shows the effect of various MeAc feed concentrations and stage cuts on the energy consumption of the PV−distillation hybrid process, where the residual stream was used as the refrigerant in the condenser. When the stage cut was within 0.4−0.45, the total energy consumption was the lowest (the mass and component balance is shown in Figure S5). This was because when the stage cut was lower than 0.3, most of the feed stream in the membrane module was recycled to column one, which increased the energy consumption. When the stage cut increased, a lower residual stream flow rate was introduced into column one, leading to a decrease in energy consumption. However, the higher stage cut suggests that a higher number of separated species were introduced into column two, resulting in MeAc with a concentration of over 99 wt %. Therefore, the energy consumption in column two increased accordingly, as shown in Figure 10b. Moreover, a higher value of the stage cut led to a higher permeate flux, and a higher vacuum pump and condensation power led to higher energy consumption during PV. The optimal energy consumption can be obtained by combining these three factors. Figure 10c also reveals that the energy consumption of the hybrid system increased with increasing MeAc concentration in the feed stream of column one. A higher concentration of MeAc in the feed stream clearly resulted in

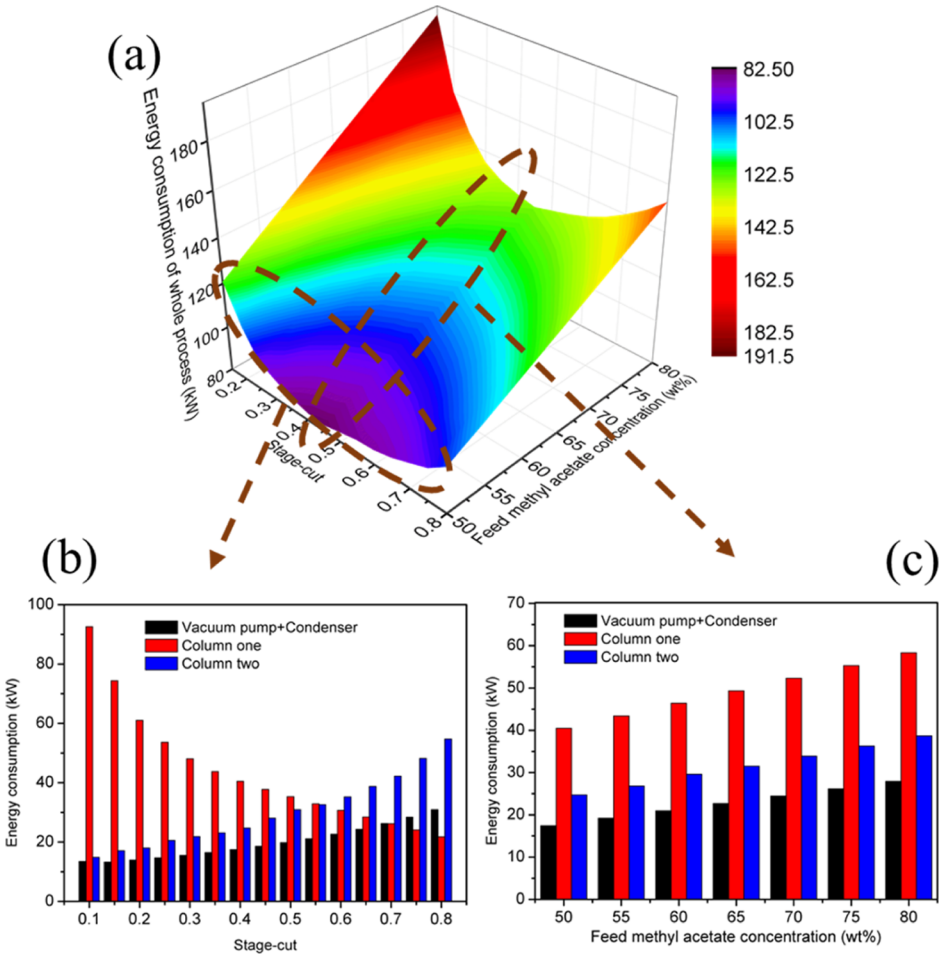

Figure 10. Effect of various MeAc feed concentrations and stage cuts on the energy consumption during the PV−distillation hybrid process (feed concentration: 50−80 wt %, stage cuts: 0.15−0.8, and feed flow rate: 100 kg/h).

https://doi.org/10.1021/acs.iecr.1c01513
Ind. Eng. Chem. Res. 2021, 60, 10327−10337

the production of a larger number of MeAc products in column two, whereas the concentration of the top stream in column two and the product remained constant. The increase in the number of products was a result of the enhancement of the feed stream at a fixed stage cut, which in turn increased the total flux of the residual stream and top stream of column one. Finally, the energy consumption in all three units increased accordingly. In addition, we considered the trace water in the feed stream. Trace water in the feed stream or residual stream did not affect the energy consumption of the entire process (the mass and component balance is shown in Figure S4).

Figure 10 reveals that the total energy consumption of the PV−distillation hybrid process (82.66 kW/100 kg) at a feed concentration of 50 wt % and a stage cut of 0.45 was considerably lower than that of special distillation. We also investigated the process by which the bottom product was used to preheat the residual stream (Figure S6);[33,43] the energy consumption was approximately 115.69/100 kg, which was higher than that of the proposed heat-integrated process in this work. The energy consumption of the PV−distillation hybrid process decreased by 24% compared to that of extractive distillation and pressurized distillation with heat integration at a MeAc feed concentration of 50 wt %. Moreover, considering that the vapor condensation from the top streams of the two columns occurred during the actual functioning of the hybrid system, the energy consumption remained low, which indicates the potential of the hybrid process with heat integration for reducing energy consumption.

3.3.3. Energy Consumption for Membranes with Various Separation Factors. Optimized process design is expected to offer outstanding benefits for energy-efficient separation. Membranes with variations in separation performance have been reported to affect the energy consumption of the entire process.[24] Therefore, membranes with separation factors within 1.5−10 were employed for simulations using the PV−distillation hybrid process. Figure 11 shows the energy consumption of the hybrid process using membranes with different separation factors at different stage cuts. As observed, the separation factor significantly affected the total energy consumption. When the separation factor was higher than 5, selectivity had little effect on the energy consumption because a higher separation factor led to a higher permeate concentration and lower fluxes of permeate and residual streams[44] (the compositions of the permeate and residual stream are shown in Figure S7) when the concentration of MeAc was fixed at the bottom of column two, as shown in Figure 12.

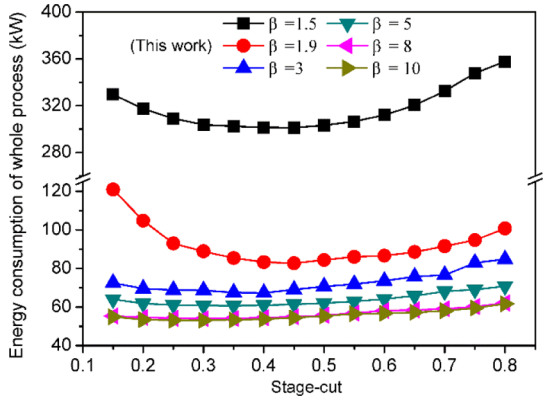

Figure 11. Energy consumption of membranes with different separation factors (β) and stage cuts (feed concentration: 50 wt %, stage cut: 0.15−0.8, and feed flow rate: 100 kg/h).

3.3.4. Energy Efficiency. Figure 13 shows the energy consumption and energy efficiency of the membranes with different separation factors. For a high separation factor, the energy efficiency of the hybrid system increased, and the increasing rate of energy efficiency gradually decreased because the energy consumption of the entire process is related to the flux fed to both columns. A high separation factor is known to result in low permeate and residual fluxes.[23,44] For a separation factor higher than 5, the flux and energy consumption slightly changed, mainly because of the slight change in permeation concentration in accordance with the mass balance.

Figure 14 compares the energy efficiencies of different processes: special distillation, pressurized distillation with heat integration, traditional hybrid process, and hybrid process with heat integration, with different feed concentrations. For the hybrid process with heat integration, an increase in the energy efficiency by 31.7% was observed, compared to that of the pressurized distillation with heat integration at a MeAc feed concentration of 50 wt %. However, the PV hybrid process with heat integration still has some weaknesses. First, the distillation process with modification shows higher thermodynamic efficiency than that of the membrane process.[45] In addition, the condensation of the permeate mixture in the PV process at 5 kPa needs cooling brine with temperature below 0 °C. Moreover, the investment cost of cooling brine is much higher than that of cooling water; extra investment will be required for the PV hybrid process with heat integration. However, with the development of membrane materials, less membrane area will be required by the hybrid process; the investment in the membrane will decrease accordingly. As shown in Figure 13, a membrane with a high separation factor can also decrease energy consumption. Therefore, the balance between energy consumption and investment cost needs further investigation, which will be published in our subsequent work.

4. CONCLUSIONS

Energy consumption is a crucial factor in separation processes and can affect the industrial feasibility. This study investigated the optimization of energy consumption in a PV−distillation hybrid process by reusing the energy of a low-temperature residual stream resulting from the vaporization enthalpy of the permeate. The temperature drop phenomenon of the residual stream was studied using simulations and experiments, which revealed that a higher stage cut led to a higher temperature drop in the residual stream. Using this information, a PV−distillation hybrid system with heat integration was designed and optimized under different operating parameters for the separation of a MeAc−MeOH azeotrope. The results showed that the PV−distillation hybrid process exhibited minimal energy consumption when the stage cut was ∼0.45. Energy savings of 24% were obtained in the hybrid process when the MeAc concentration in the feed stream was 50 wt %, compared to the energy consumption via pressurized distillation with heat integration. Additionally, the hybrid process was found to increase the energy efficiency by 31.7% compared to that of the pressurized distillation with heat integration. Membranes with various separation factors were also investigated, and the results revealed that a higher separation factor led to lower energy consumption and higher energy efficiency in the hybrid

https://doi.org/10.1021/acs.iecr.1c01513
Ind. Eng. Chem. Res. 2021, 60, 10327−10337

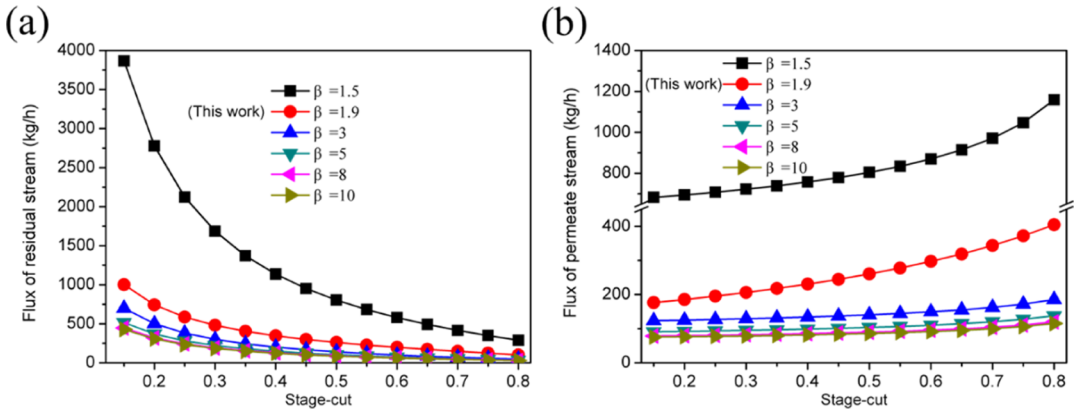

Figure 12. Fluxes of (a) residual and (b) permeate streams in various processes and stage cuts (feed concentration: 50 wt %, stage cut: 0.15−0.8, and feed flow rate: 100 kg/h).

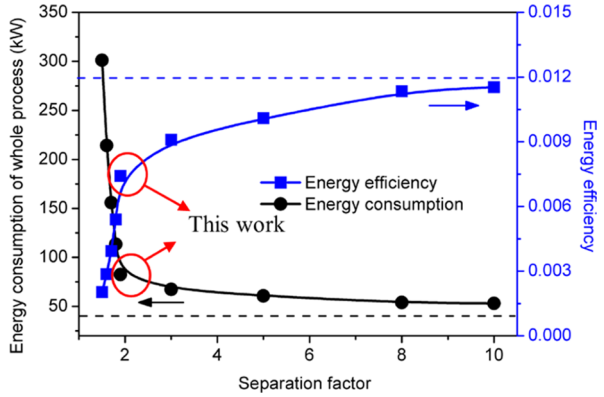

Figure 13. Effect of separation factors on energy efficiency and energy consumption of the entire process.

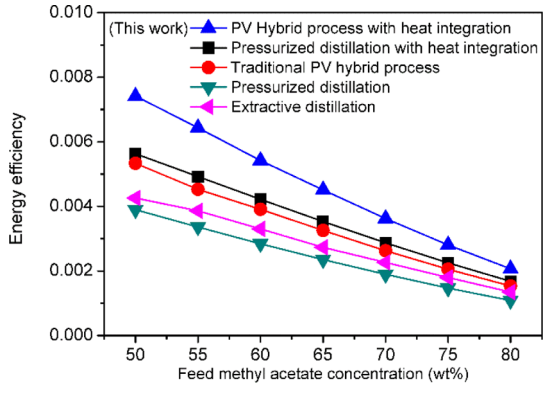

Figure 14. Energy efficiencies of different processes with varied feed concentrations.

process. However, when the separation factor was higher than 5, the rate of increase in energy efficiency slowed and stabilized. Therefore, membrane performance and process design are critical for improving the energy efficiency of hybrid processes for the separation of azeotropic mixtures.

■ ASSOCIATED CONTENT

Supporting Information

The Supporting Information is available free of charge at https://pubs.acs.org/doi/10.1021/acs.iecr.1c01513.

Calculation process of separation performance; model of the PV process; heat transfer with environment; flowsheet of the pressurized distillation process with heat integration; mass balance of the hybrid process with trace water; mass balance of the PV−distillation hybrid process; energy consumption of the PV−distillation hybrid process; mass flow of residual and permeate streams of membrane with different separation factors; regression data of parameters; and NRTL binary parameters (PDF)

■ AUTHOR INFORMATION

Corresponding Authors

Haoli Zhou − *State Key Laboratory of Materials-Oriented Chemical Engineering, College of Chemical Engineering, Nanjing Tech University, Nanjing 210009, PR China;* orcid.org/0000-0003-4699-5325; Email: zhouhl@njtech.edu.cn

Wanqin Jin − *State Key Laboratory of Materials-Oriented Chemical Engineering, College of Chemical Engineering, Nanjing Tech University, Nanjing 210009, PR China;* orcid.org/0000-0001-8103-4883; Phone: +86-25-83172272; Email: wqjin@njtech.edu.cn; Fax: +86-25-83172272

Authors

Chuanxin Zong − *State Key Laboratory of Materials-Oriented Chemical Engineering, College of Chemical Engineering, Nanjing Tech University, Nanjing 210009, PR China*

Qingkai Guo − *State Key Laboratory of Materials-Oriented Chemical Engineering, College of Chemical Engineering, Nanjing Tech University, Nanjing 210009, PR China*

Bowen Shen − *State Key Laboratory of Materials-Oriented Chemical Engineering, College of Chemical Engineering, Nanjing Tech University, Nanjing 210009, PR China*

Xiaoquan Yang − *State Key Laboratory of Materials-Oriented Chemical Engineering, College of Chemical Engineering, Nanjing Tech University, Nanjing 210009, PR China*

Complete contact information is available at: https://pubs.acs.org/10.1021/acs.iecr.1c01513

Author Contributions

C.Z.: Experimental executor, experimental analysis, discussion, and writing—original draft. Q.G.: Experimental analysis and discussion. B.S.: Experimental analysis and discussion. X.Y.: Experimental analysis and discussion. H.Z.: Project administration, supervision, experimental analysis, funding acquis-

https://doi.org/10.1021/acs.iecr.1c01513
Ind. Eng. Chem. Res. 2021, 60, 10327−10337

ition, validation, writing—original draft, and writing—review and editing. W.J.: Project administration, supervision, experimental analysis, funding acquisition, validation, writing—original draft, and writing—review and editing.

Notes

The authors declare no competing financial interest.

■ ACKNOWLEDGMENTS

This work was supported by the National Key Research and Development Program of China (no. 2017YFC0210901), Six Talent Peaks Project in Jiangsu Province (JNHB-041), the Fund of State Key Laboratory of Materials-Oriented Chemical Engineering (ZK201715), and the Top-notch Academic Programs Project of Jiangsu Higher Education Institutions (TAPP).

■ NOMENCLATURE

A	membrane area (m^2)
J	membrane flux ($kg/(h \cdot m^2)$)
m	mass (kg)
p	pressure (kPa)
β	separation factor: (-)
c	capacity heat (J/(kg·K))
R	ideal gas constant (kJ/(kmol·K))
Δt	time interval: (h)
Q_i	heat duty (kW)
T	temperature (°C)
F	total flux of stream (kg/h)
W	energy requirement: (kW)
H	enthalpy (J)
P_S	specific energy requirement (kJ/mol)
γ	activity coefficient: (-)
A, B, C, a, n	regression coefficients (-)
q_V	volume flow (l/h)
w	weight fraction (kg/kg)
x	molar fraction in the liquid phase (mol/mol)
y	molar fraction in the vapor phase (mol/mol)
k	isentropic coefficient (-)
η	energy efficiency: (-)

■ INDICES

f	feed side of the membrane
i, j	component i, j
p	permeate side of the membrane
r	residual side of the membrane
in, out	inlet and outlet stream of the vacuum pump
MeAc	methyl acetate
MeOH	methanol
vap	vaporization

■ REFERENCES

(1) Sholl, D. S.; Lively, R. P. Seven chemical separations to change the world. *Nature* **2016**, *532*, 435−437.
(2) Sekulic, J.; Elshof, J.; Blank, D. Separation mechanism in dehydration of water/organic binary liquids by pervaporation through microporous silica. *J. Membr. Sci.* **2005**, *254*, 267−274.
(3) Figueroa Paredes, D. A.; Laoretani, D. S.; Zelin, J.; Vargas, R.; Vecchietti, A. R.; Espinosa, J. Screening of pervaporation membranes for the separation of methanol-methyl acetate mixtures: An approach based on the conceptual design of the pervaporation-distillation hybrid process. *Sep. Purif. Technol.* **2017**, *189*, 296−309.
(4) Kárászová, M.; Sedláková, Z.; Friess, K.; Izák, P. Effective permeability of binary mixture of carbon dioxide and methane and pre-dried raw biogas in supported ionic liquid membranes. *Sep. Purif. Technol.* **2015**, *153*, 14−18.
(5) Del Pozo Gomez, M. T.; Klein, A.; Repke, J.-U.; Wozny, G. A new energy-integrated pervaporation distillation approach. *Desalination* **2008**, *224*, 28−33.
(6) Bausa, J.; Marquardt, W. Shortcut design methods for hybrid Membrane/Distillation processes for the separation of nonideal multicomponent mixtures. *Ind. Eng. Chem. Res.* **2000**, *39*, 1658−1672.
(7) Del Pozo Gomez, M. T.; Repke, J.-U.; Kim, D.-y.; Yang, D. R.; Wozny, G. Reduction of energy consumption in the process industry using a Heat-Integrated hybrid distillation pervaporation process. *Ind. Eng. Chem. Res.* **2009**, *48*, 4484−4494.
(8) Byrne, F. P.; Jin, S.; Paggiola, G.; Petchey, T. H. M.; Clark, J. H.; Farmer, T. J.; Hunt, A. J.; Robert Mcelroy, C.; Sherwood, J. Tools and techniques for solvent selection: Green solvent selection guides. *Sustainable Chem. Processes* **2016**, *4*, 7.
(9) Wang, Y.; Liao, J.; Zhang, J.; Wang, S.; Zhao, Y.; Ma, X. Hydrogenation of methyl acetate to ethanol by Cu/ZnO catalyst encapsulated in SBA-15. *AIChE J.* **2017**, *63*, 2839−2849.
(10) Wang, G.; Li, Z.; Li, C.; Zhang, S. Preparation of methyl acrylate from methyl acetate and methanol with mild catalysis of cobalt complex. *Chem. Eng. J.* **2019**, *359*, 863−873.
(11) Li, F.; Chen, B.; Huang, Z.; Lu, T.; Yuan, Y.; Yuan, G. Sustainable catalysts for methanol carbonylation. *Green Chem.* **2013**, *15*, 1600−1607.
(12) Patil, P. D.; Reddy, H.; Muppaneni, T.; Deng, S. Biodiesel fuel production from algal lipids using supercritical methyl acetate (glycerin-free) technology. *Fuel* **2017**, *195*, 201−207.
(13) Li, B.; Xu, J.; Han, B.; Wang, X.; Qi, G.; Zhang, Z.; Wang, C.; Deng, F. Insight into Dimethyl Ether Carbonylation Reaction over Mordenite Zeolite from in-Situ Solid-State NMR Spectroscopy. *J. Phys. Chem. C* **2013**, *117*, 5840−5847.
(14) Park, S. Y.; Shin, C.-H.; Bae, J. W. Selective carbonylation of dimethyl ether to methyl acetate on Ferrierite. *Catal. Commun.* **2016**, *75*, 28−31.
(15) Kirbaslar, Ş. I.; Terzioglu, H.; Dramur, U. Catalytic esterification of methyl alcohol with acetic acid. *Chin. J. Chem. Eng.* **2001**, *9*, 90−96.
(16) Gmehling, J.; Onken, U.; Arlt, W. *Vapor−Liquid Equilibrium Data Collection*; Dechema: Frankuurt, 1977.
(17) Zhu, Z.; Geng, X.; He, W.; Chen, C.; Wang, Y.; Gao, J. Computer-Aided screening of ionic liquids as entrainers for separating methyl acetate and methanol via extractive distillation. *Ind. Eng. Chem. Res.* **2018**, *57*, 9656−9664.
(18) Suárez, F.; Urtubia, R. Tackling the water-energy nexus: An assessment of membrane distillation driven by salt-gradient solar ponds. *Clean Technol. Environ. Policy* **2016**, *18*, 1697−1712.
(19) Steinigeweg, S.; Gmehling, J. Transesterification processes by combination of reactive distillation and pervaporation. *Chem. Eng. Process.* **2004**, *43*, 447−456.
(20) Xu, H.; Wang, X.; Zou, Y.; Wang, L. Exergy, economic and environmental assessment of sec-butyl acetate hydrolysis to sec-butyl alcohol using a combined reaction and extractive distillation system. *Fuel* **2021**, *286*, 119372.
(21) Arpornwichanop, A.; Sahapatsombud, U.; Patcharavorachot, Y.; Assabumrungrat, S. Hybrid process of reactive distillation and pervaporation for the production of tert-amyl ethyl ether. *Chin. J. Chem. Eng.* **2008**, *16*, 100−103.
(22) Harvianto, G. R.; Ahmad, F.; Nhien, L. C.; Lee, M. Vapor permeation−distillation hybrid processes for cost-effective isopropanol dehydration: Modeling, simulation and optimization. *J. Membr. Sci.* **2016**, *497*, 108−119.
(23) Harvianto, G. R.; Ahmad, F.; Lee, M. A thermally coupled reactive distillation and pervaporation hybrid process for n -butyl acetate production with enhanced energy efficiency. *Chem. Eng. Res. Des.* **2017**, *124*, 98−113.
(24) Castel, C.; Favre, E. Membrane separations and energy efficiency. *J. Membr. Sci.* **2018**, *548*, 345−357.

https://doi.org/10.1021/acs.iecr.1c01513
Ind. Eng. Chem. Res. 2021, 60, 10327−10337

(25) Li, Y.; Zong, C.; Zhou, H.; Jin, W. Pervaporative separation of methyl acetate−methanol azeotropic mixture using high-performance polydimethylsiloxane/ceramic composite membrane. *Asia-Pac. J. Chem. Eng.* **2019**, *14*, No. e2343.
(26) Lux, S.; Winkler, T.; Körbler, M.; Siebenhofer, M. Assessment of pervaporative separation of methyl acetate and methanol using organophilic membranes. *Chem. Eng. Sci.* **2017**, *158*, 507−515.
(27) Zong, C.; Yang, X.; Chen, D.; Chen, Y.; Zhou, H.; Jin, W. Rational tuning of the viscosity of membrane solution for the preparation of sub-micron thick PDMS composite membrane for pervaporation of ethanol-water solution. *Sep. Purif. Technol.* **2021**, *255*, 117729.
(28) Lux, S.; Winkler, T.; Forstinger, M.; Friesenbichler, S.; Siebenhofer, M. Pervaporative separation of Methanol-Methyl acetate mixtures with commercial PVA membranes. *Sep. Sci. Technol.* **2015**, *50*, 2920−2929.
(29) Rom, A.; Miltner, A.; Wukovits, W.; Friedl, A. Energy saving potential of hybrid membrane and distillation process in butanol purification: Experiments, modelling and simulation. *Chem. Eng. Process.* **2016**, *104*, 201−211.
(30) Huttunen, M.; Nygren, L.; Kinnarinen, T.; Häkkinen, A.; Lindh, T.; Ahola, J.; Karvonen, V. Specific energy consumption of cake dewatering with vacuum filters. *Miner. Eng.* **2017**, *100*, 144−154.
(31) Farshad, F.; Iravaninia, M.; Kasiri, N.; Mohammadi, T.; Ivakpour, J. Separation of toluene/n-heptane mixtures experimental, modeling and optimization. *Chem. Eng. J.* **2011**, *173*, 11−18.
(32) Vallieres, C.; Favre, E.; Arnold, X.; Roizard, D. Separation of binary mixtures by dense membrane processes: Influence of inert gas entrance under variable downstream pressure conditions. *Chem. Eng. Sci.* **2003**, *58*, 2767−2775.
(33) Andre, A.; Nagy, T.; Toth, A. J.; Haaz, E.; Fozer, D.; Tarjani, J. A.; Mizsey, P. Distillation contra pervaporation: Comprehensive investigation of isobutanol-water separation. *J. Cleaner Prod.* **2018**, *187*, 804−818.
(34) Saghatoleslami, N.; Vatankhah, G. H.; Karimi, H.; Noie, S. H. Prediction of the overall sieve tray efficiency for a group of hydrocarbons, an artificial neural network approach. *J. Nat. Gas Sci. Eng.* **2011**, *3*, 319−325.
(35) Liu, J.; Yang, B.; Lu, S.; Yi, C. Multi-scale study of reactive distillation. *Chem. Eng. J.* **2013**, *225*, 280−291.
(36) Haelssig, J. B.; Tremblay, A. Y.; Thibault, J. A new hybrid membrane separation process for enhanced ethanol recovery: Process description and numerical studies. *Chem. Eng. Sci.* **2012**, *68*, 492−505.
(37) Ceylan, İ.; Yilmaz, S.; İnanç, Ö.; Ergün, A.; Gürel, A. E.; Acar, B.; İlker Aksu, A. Determination of the heat transfer coefficient of PV panels. *Energy* **2019**, *175*, 978−985.
(38) Matsumura, M.; Kataoka, H.; Sueki, M.; Araki, K. Energy saving effect of pervaporation using oleyl alcohol liquid membrane in butanol purification. *Bioprocess Biosyst. Eng.* **1988**, *3*, 93−100.
(39) Zhang, Z.; Zhang, Q.; Li, G.; Liu, M.; Gao, J. Design and control of methyl acetate-methanol separation via heat-integrated pressure-swing distillation. *Chin. J. Chem. Eng.* **2016**, *24*, 1584−1599.
(40) Neti, N. R.; Parmar, G. R.; Bakardjieva, S.; Subrt, J. Thick film titania on glass supports for vapour phase photocatalytic degradation of toluene, acetone, and ethanol. *Chem. Eng. J.* **2010**, *163*, 219−229.
(41) Genduso, G.; Amelio, A.; Colombini, E.; Luis, P.; Degrève, J.; Van der Bruggen, B. Retrofitting of extractive distillation columns with high flux, low separation factor membranes: A way to reduce the energy demand? *Chem. Eng. Res. Des.* **2016**, *109*, 127−140.
(42) Zheng, H.; Xie, L.; Cai, L.; Wu, D.; Zhao, S. Recovery of PVA by-product methyl acetate via reactive and extractive distillation. *Chem. Eng. Process.* **2015**, *95*, 214−221.
(43) Haaz, E.; Szilagyi, B.; Fozer, D.; Toth, A. J. Combining extractive heterogeneous-azeotropic distillation and hydrophilic pervaporation for enhanced separation of non-ideal ternary mixtures. *Front. Chem. Sci. Eng.* **2020**, *14*, 913−927.
(44) Harvianto, G. R.; Ahmad, F.; Lee, M. A hybrid reactive distillation process with high selectivity pervaporation for butyl acetate production via transesterification. *J. Membr. Sci.* **2017**, *543*, 49−57.
(45) Demirel, Y. Thermodynamic analysis of separation systems. *Sep. Purif. Technol.* **2004**, *39*, 3897−3942.

https://doi.org/10.1021/acs.iecr.1c01513
Ind. Eng. Chem. Res. 2021, 60, 10327−10337